THE JOURNAL OF THE ACOUSTICAL SOCIETY OF KOREA Vol.22, No.3E 2003. 9. pp. 133~140

Time Series Simulation of Explosive Charges in Shallow Water Using Ray Approach

Jooyoung Hahn*, Seongwook Lee*, Jungyul Na*
*Department of Earth and Marine Sciences, Hanyang University
(Received July 4 2003; accepted September 17 2003)

Abstract

A time series simulation is presented by a ray approach for the simulating the received waveform of a broadband acoustical signals interacting with the ocean boundaries. The environment is assumed to be horizontally stratified, and the seafloor is described in terms of homogeneous fluid half-space. The ray approach includes the effects of reflection from the air-water, water-sediment interface and phase shifts due to boundaries interaction. To generate time series, we assume that the acoustic energy propagates from source to receiver along eigenrays and represent the action of the bottom on the incident wave by a linear filter and characterized in the frequency domain by the transfer function. As example application, the time series for an explosive source in a shallow water environment is calculated and analyzed in terms of acoustical process. good agreement with measured time series is demonstrated.

Keywords: *Broadband signal processing, Complex reflection coefficient, Hilbert transform, Phase shift, Eigenray, Geoacoustic parameter*

I. Introduction

This article develops a ray approach for simulating the propagation of broadband signals with the effects of the boundaries in a shallow water environment having fluid bottom. The method mainly relies on the inclusion of phase shift in ray trajectories due to the total reflection from the seafloor.

Acoustic waves generated by a point source in the ocean may be reflected due to total internal reflection at incident angle greater than the critical angle[1]. In the case of total reflection, an incident wave suffers a phase change and retardation in time that is inversely proportional to the frequency. Thus, the various Fourier components of the incident pulse experience phase lag by different amounts and the reflected pulse will have a different shape[2]. With the virtual reflector concept, the sound propagation into the real interface produces a beam displacement caused by reflection beyond the critical angle[1].

Historically, propagation in shallow water has been studied primarily using normal mode theory. Recently, it has been found that if beam displacement is included, ray theory can also predict valid results in shallow water environment[3].

The ability to simulate broadband signals reflected from a seafloor would be a valuable tool in the analysis of experimental data used to estimate seafloor structure and geoacoustic parameters. Comparison of simulated and measured signals would be also valuable in guiding theoretical research by clearly identifying unexplained characteristics of bottom interaction[4]. From the comparison of the transmission loss and time series, the best

Corresponding author: Jooyoung Hahn (jyhahn@ihanyang.ac.kr)
Department of Earth and Marine Sciences, Hanyang University
Dep. of Earth and Marine Sciences, Hanyang University, Sa-1-Dong, Sang-Rok-Gu, Ansan, Korea

estimate geoacoustic parameters can be selected inversely.

To generate time series, it is assumed that acoustic energy propagates from source to receiver along eigenrays and represent the action of the bottom on the incident wave by a linear filter and characterized in the frequency domain by the transfer function. The contribution of each eigenray to the received time series can be calculated individually and then the contributions of all the rays are put together to give the total time series. The bottom-bounce waveform is constructed from the Hilbert transform of the incident unit waveform and the complex envelope signal.

This article is organized as follows. Section I summarizes the equations governing phase shift and explains the method for obtaining the reflected pulse directly through the frequency domain. In Section II explains the explosive waveform measured in this experiment and shows its distorted waveform by bottom reflection. The method for simulating time series, which involves treating the frequency dependence of eigenrays having phase shift is covered in section III. Details of a typical simulation are given in this section. This method is demonstrated in section IV by comparing simulations against actual time series measured in the Chejoo-97 experiment having shallow water overlying a silty-sand bottom. Finally, conclusions are contained in section V.

II. Total Reflection and Phase Distortion at Fluid Interface

When a single-frequency plane wave strikes an interface between two fluid media and there is no attenuation in the media, a phase shift of the reflected wave occurs if the angle of incidence is greater than the critical angle for the media. For sound incident from the water to a sediment bottom, when $c_2>c_1$, there is the possibility of "total reflection". Total reflection occurs at angle of incidence $\theta_1 \geq \theta_c$, where θ_c is "critical angle"[1]. Here θ_1 is the angle of incidence measured from the normal to the bottom and c_1, c_2 are sound velocities.

$$\theta_c = \arcsin(c_1/c_2), \quad c_2 > c_1 \tag{1}$$

For angles greater than critical, the reflection coefficient $\Re$ is

$$\Re = e^{2i\phi} \tag{2}$$

Where ϕ depends only on the angle of incidence θ_1

$$\phi = \arctan \frac{\left[\sin^2\theta_1 - (c_1/c_2)^2\right]^{\frac{1}{2}}}{(\rho_2/\rho_1)\cos\theta_1} \tag{3}$$

Here ρ_1, ρ_2 are densities. The indices 1 and 2 refer, respectively, to the incident medium and the bottom. This phase shift 2ϕ is a function of the ratio of density and sound velocity of the two media and the angle of incidence. Although this phase shift is independent of the frequency of the incident pulse, the reflected pulse shape can be significantly distorted and its peak amplitude altered[5].

It is convenient to represent the action of the bottom on the incident wave by a linear filter, characterized in the frequency domain by the transfer function[5]

$$H(f) = \begin{cases} \exp(2i\phi), f > 0 \\ \exp(-2i\phi), f < 0 \end{cases} \tag{4}$$

If the spectrum of the incident pulse is

$$X(f) = \int_{-\infty}^{\infty} x(t)\exp(-i2\pi ft)dt \tag{5}$$

then the spectrum of the reflected pulse is

$$Y(f) = H(f)X(f) = \exp[i2\phi\,\mathrm{sgn}(f)]X(f) \tag{6}$$

Therefore, since a time waveform $x(t)$, impulse response $h(t)$ and reflected wave $y(t)$ are all real, the received pressure time series is inverse Fourier transform of the product of frequency response and the source spectrum

$$\begin{aligned} y(t) &= \int_{-\infty}^{\infty} X(f)\exp(i2\pi ft)df \\ &= \mathrm{Re}\{[x(t) + ix_H(t)]\exp(i2\phi)\} \end{aligned} \tag{7}$$

Here, $x_H(t)$ is the Hilbert transform of $x(t)$[6].

Equation (7) represents the method of obtaining the

reflected pulse, directly through the frequency domain. 2ϕ is the phase shift upon reflection and is given in Equation (2).

III. The Explosive Charges and Phase Distortion Caused by Bottom Reflection

3.1. The Waveform of an Underwater Explosion

A typical example of the explosive waveform measured in this experiment is shown in Figure 1 and the energy density spectrum for this charge is presented in Figure 2. The sound source was a 0.031 Kg Tetryl charge detonated at depth of 18m. The signal was recorded at a distance of 100 m from the source by a hydrophone at a depth of 33 m. The waveform consists of a shock wave followed by a series of bubble pulses and it has been truncated after two bubble pulses to eliminate the surface reflection.

In Figure 2, the thick solid curve is the combined spectrum of shock wave and first two bubble pulses. The interference between the shock wave and bubble pulses produces a modulated energy spectrum with a moderately broad peak near the bubble frequency 20 Hz. At the higher frequencies (above 200 Hz), the combined spectrum is given by simple energy addition and is dominated by the shock wave, at low frequencies(20-150 Hz), the combined spectrum falls off with decreasing frequency owing to phase cancellation of shock wave and bubble pulses. However, the contribution of second bubble pulse is negligible.

3.2. Phase Distortion Caused by Bottom Reflection

As we represent the action of the bottom by a linear filter, for the superposition condition[7], the linearly combined input signals - shockwave and two bubble pulses, must produce the linearly combined output.

$$y(t) = y_{shockwave}(t) + y_{1st\_bubble\_pulse}(t) + y_{2nd\_bubble\_pulse}(t) \quad (8)$$

To see the phase-shifted waveform, we have allowed arbitrary starting and ending times for the shockwave and bubble pulses and an arbitrary phase shift for the each carrier in bubble pulses. We employ the approach of equation (7) and Hilbert transform for this example to find the reflected unit waveform $y(t)$

$$y(t) = \mathrm{Re}\{[x(t) + ix_H(t)]\exp(i2\phi)\} \quad (9)$$

Figure 3 presented the curve of the simulated reflected waveform for the incident wave, $\phi = \pi/3$.

At the beginning of the phase-shifted waveform, the precursor corresponds to a "refracted" or "lateral" wave traveling through the higher speed $z<0$ half-space. For a source at a finite distance -spherical waves, it proceeds the

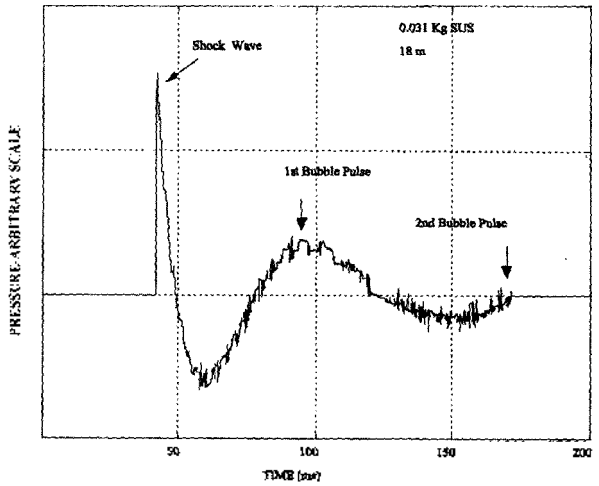

Figure 1. Waveform from the explosion of a 0.031 Kg charge at a depth of 18 m.

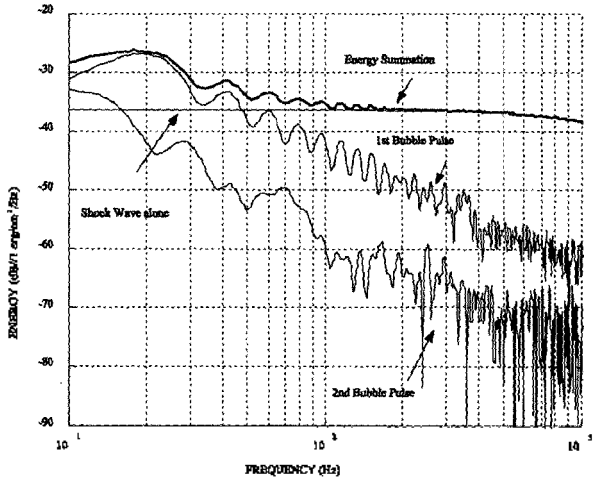

Figure 2. Energy density spectrum of a 0.031 Kg charge at a depth of 18 m.

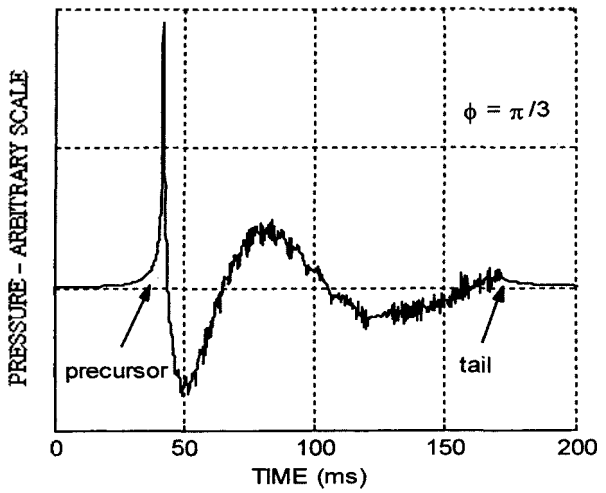

Figure 3. Simulated phase-shifted waveform, showing precursor and tail ($\phi = \pi/3$).

reflected arrival by a finite amount but, in the case of a "plane" wave, the source has been removed to infinity and the refracted wave proceeds the reflected arrival by an infinite amount, the precursor should be ignored entirely [2]. And even just after the second bubble pulse is eliminated in input waveform, there is a large delay of low frequency components tail. The tail indicated by equation $\tau = 2(n\pi + \phi)/\omega$, n is a constant. Due to the phase-shifted waveform overlaps two lobes of the sinusoid, a slight distortion occurs near the bubble pulses. Near the shockwave, there is still significant distortion. In our ray approach, we neglect reconversion of energy from shear waves in the sediment.

IV. Ray Approach for a Homogeneous Fluid Half-space Model

To develop the ray approach, it is assume that the acoustic energy propagates from source to receiver along eigenrays. The trajectories of the eigenrays are independent of frequency and are determined completely by the sound-speed structure via Snell's law and reflection from the boundaries. Moreover, the linear system is assumed. This means that the contribution of each eigenray to the received time series can be calculated individually and then the contributions of all the rays are

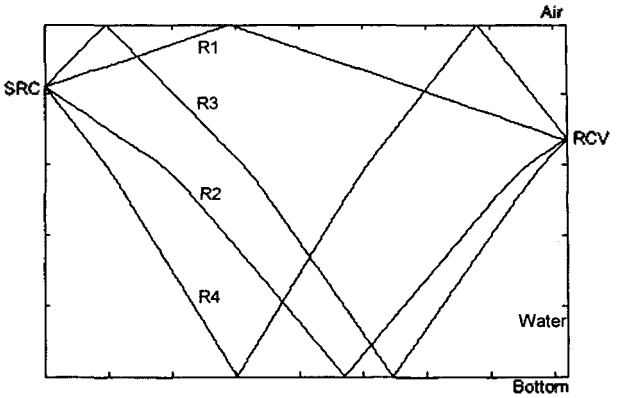

Figure 4. Four types of possible single bottom interaction eigenrays.

put together to give the total time series.

Only caring about the eigenrays which incident angles greater than the critical, we integrate rays that interact with bottom just once. Additional ray paths representing multiple reflections are not included in our ray approach. Figure 4 illustrates four types of possible single boundary interaction eigenrays (R1-R4).

The ray theoretical pressure transmission function response at the receiver for a delta function source in time and space for the multiple arrivals in this horizontally stratified ocean environment is

$$p(t) = \int_{-\infty}^{\infty} df e^{2\pi i f t} \tilde{p}(f) \tag{10}$$

Where the eigenray frequency response $\tilde{p}(f)$ is a superposition of the frequency response of each eigenray.

$$\tilde{p}(f) = \sum_{j=1}^{n} P_j Q_j e^{-i2\phi_j} e^{-2\pi i f t_j} e^{-2\pi f A_j} \tag{11}$$

Here, the summation index j denotes the j^{th} eigenray. and P_j are t_j the geometrical divergence and the travel time for the jth ray, respectively. In addition, Q_j represents the accumulation of interface reflection and transmission coefficients along the j^{th} ray and $2\pi f A_j$ is the attenuation occurring in the sediment. All of eigenrays are totally reflected and no sound transmitted to the sediment, the term $2\pi f A_j$ would be 0, Q_j would be unity for each eigenray. For angles greater than critical, the magnitude of the reflection coefficient is 1. The frequency

independent phase shift 2 ϕ_j, accumulates the phase shifts due to reflection from the water-air and water-sediment interfaces. For each bounce off the water-air interface, a phase shift of π is assigned, since the reflected pressure is the negative of the incident pressure. Equation (9) explicitly shows the simple frequency dependence of $\tilde{p}(f)$ in the two exponential factors. All other terms are independent of frequency.

The basic numerical approach to the simulation of a received time waveform is carried out as follows : The sound-speed structure of the water column, along with the geometry of the source and receiver, are input to a computer program which find the eigenrays [8], calculates the travel times, finds the incident angles and calculates phase shifts due to reflections from the boundaries. This information is used to construct the frequency response. The inverse Fourier transform of the product of frequency response and the source spectrum is performed numerically using the fast Fourier transform to calculate the received time domain response at the receiver. The complete received time series is the sum of the responses of all the eigenrays.

Figure 5 is an example of the simulated received signal calculated by using the ray approach as explained above.

For this example, the depths of the source and receiver are 18 m, 38 m respectively and the receiver is 820 m away from the source. The bottom depth is 104 m and the sediment type is silty-sand (density 1800 kgm^{-3}, sound speed 1650 m/s[9]). The phase shift of the incident wave due to bottom interaction is in Figure 6. It is calculated by the Equation (3). The water sound speed profile, shown in Figure 7, is used measured sound speed profile in experiment.

In order to understand the characteristic of the simulated waveform, the signals due to the individual eigenrays and arrival structures are shown in Figure 8 and Figure 9.

All of the rays are of a total reflecting type because the angles of incident are greater than the critical as shown in Figure 6. For this sound-speed structure and geometry, negative sound-speed gradient (Figure 7) produces a ray curvature that bends downward toward to the bottom so that direct path to the receiver does not exist and the

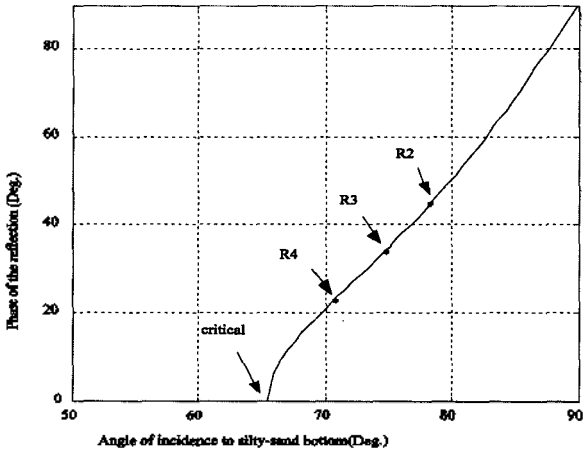

Figure 6. Imaginary phase of reflection coefficient at the water-sediment interface (density 1800 kgm^{-3}, sound speed 1650 m/s).

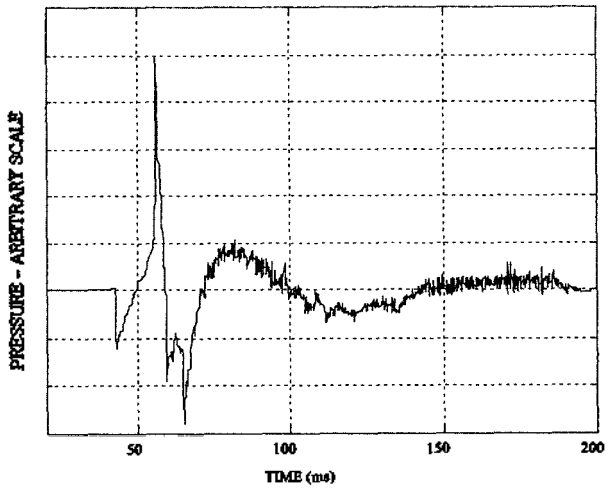

Figure 5. Example of the simulated received signal.

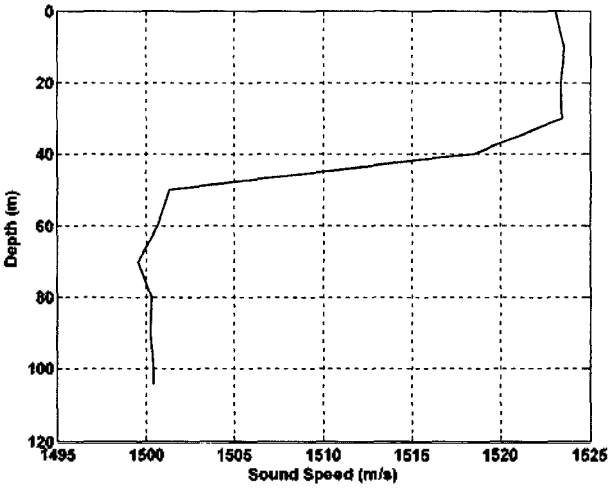

Figure 7. Measured soundspeed profile for water column.

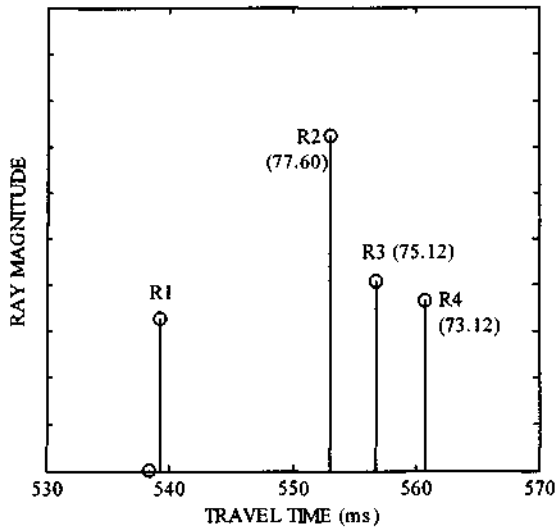

Figure 8. Computed arrival times of rays. The peaks are identified by the each eigenray and incident angle to the bottom. The height of stem represents the ray magnitude.

bottom reflected ray (R2) makes the larger contribution than surface reflected ray (R1) even path length is longer, shown in Figure 8. The specular ray with a single water-air reflection (R1) produces an inverted waveform because of the π phase shift and due to the complex plane wave reflection coefficient at the water-sediment interface, the specular ray with water-sediment reflection (R2) produces phase shifted waveform according to the amount of angle of incident. The Eigenrays R3, R4 interact with both surface and bottom once so they have a total phase shift $\pi+\phi_R$. A superposition of the signals in Figure 9 gives us the complete received waveform shown in Figure 5. Note that single bottom reflected ray in Figure 9 (R2) carries most of the energy compared to other rays.

V. Comparison of Measured and Simulated Time Series

This section demonstrates the accuracy of the ray approach presented above and the ability to describe the effect of the seafloor on a broadband acoustic signal.

The pressure time series was measured in the South Sea, 18 km away from the Chejoo island to the west. The water

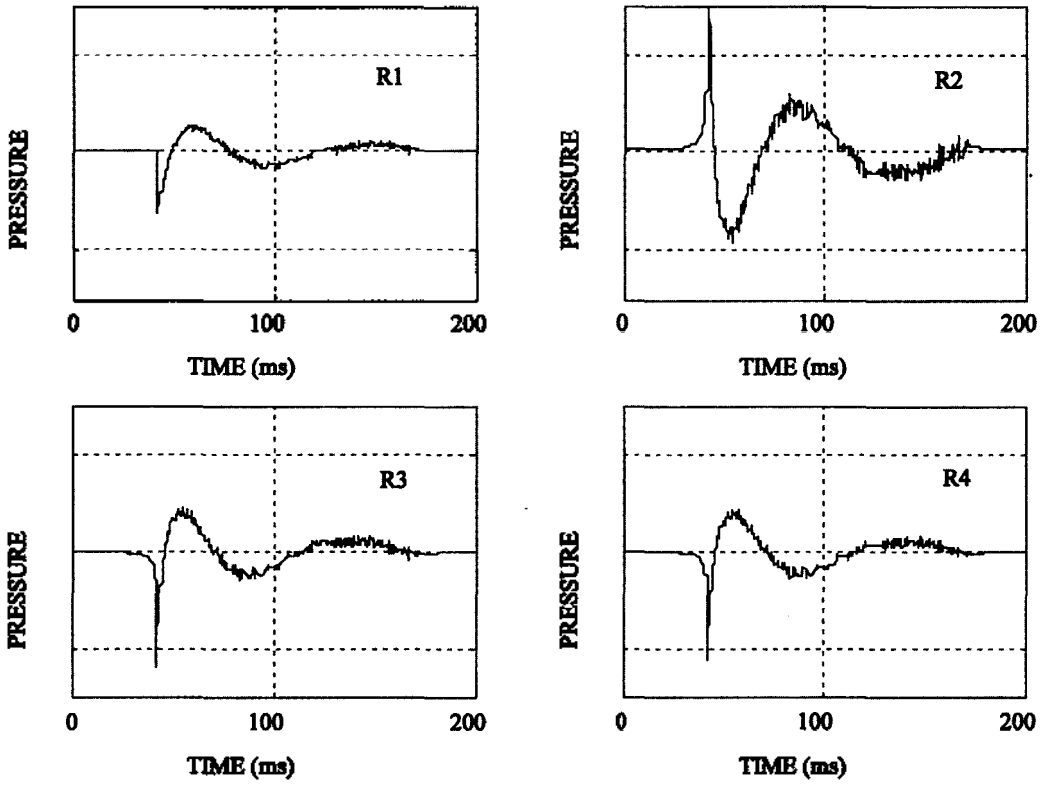

Figure 9. Reflected waveform for a given unit waveform shown in Figure 1.

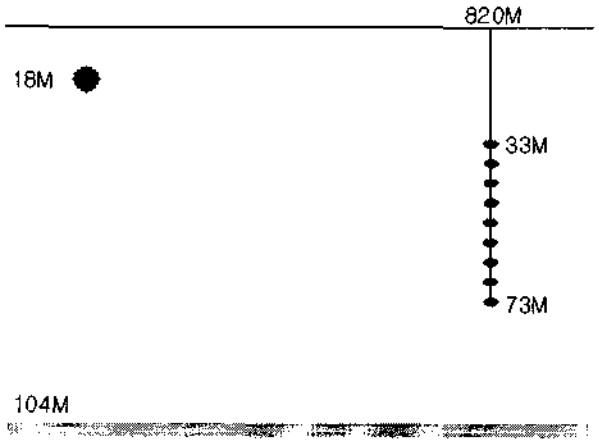

Figure 10. Geometry of the Chejoo-97 experiment.

depth is about 104 m and the sediment in this area is classified as silty-sand[9]. The sound source was a 1.1 Oz Tetryl charge detonated at depth of 18 m. The signal was recorded at a distance of 820 m from the source by a vertical line array with 9 hydrophones at depth of 33 m to 73 m with space of 5 m. The geometry of the experiment is shown in Figure 10.

The input sediment type and the measured sound speed profile of the water column used to simulate the time series are explained in section III. The acoustic parameters for sediment were obtained from the published work of Hamilton[10] and the source spectrum was obtained from the measured time series. In section 3.1 and 3.2, the detail of the unit waveform and source spectrum is described.

The ray paths reflecting the bottom once are all total reflecting rays for the experimental geometry. Figure 11 presents a comparison of the measured and simulated time series in the 10 - 500 Hz band. The agreement between experiment and theory is reasonable.

The four reflected rays are clearly identified on the basis of the distortion of the shock wave and bubble pulses. The first reflected arrival in Figure 11 (42 - 55 ms) are inverted, since it has a single water-air reflection [see Figure 9-R1]. The next reflected arrival (55 - 59 ms) has no water-air reflections[see Figure 9-R2]. Finally, the last two reflected arrivals (59 - 67 ms) have both water-air and water-bottom reflections[see Figure 9-R3, R4]. Note that the direct arrival does not exist due to the strong negative sound-speed gradient.

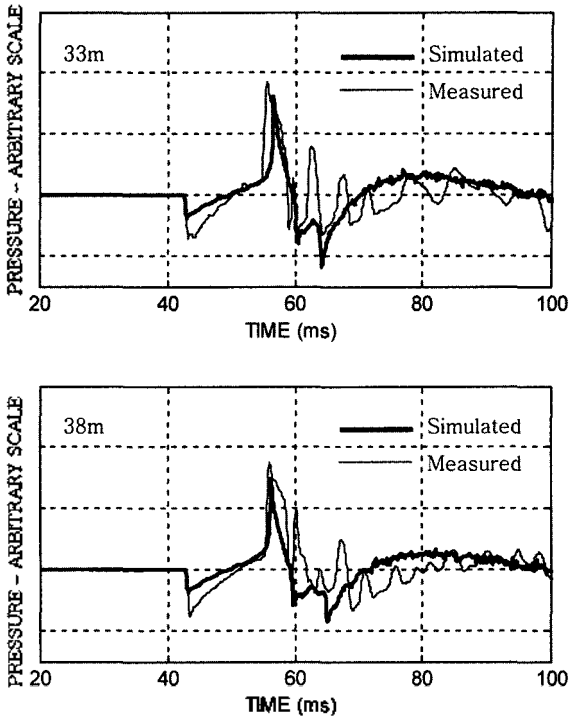

Figure 11. Comparison of simulated and measured time series, 10-500 Hz frequency band. Double solid lines are simulated and solid lines are measured signal. Receiver depths in 33 m and 38 m.

VI. Conclusion

In this study, a ray approach for simulating bottom interacting broadband signals was developed. To generate time series, we assume that the acoustic energy propagates from source to receiver along eigenrays and represent the action of the bottom on the incident wave by a linear filter and characterized in the frequency domain by the transfer function. The bottom-bounce waveform is constructed from the Hilbert transform of the incident unit waveform and the complex envelope signal.

The major limitation of the ray approach presented here is the limitation to sediment to fluid half-space and no attenuation in sediment layer. We also neglect reconversion of energy from shear waves in the sediment. But it is possible to use of multiple layer of ocean bottom and a geoacoustic profile that allow the sediment to be treated as part of the propagation medium, with ray paths both reflected from the sediment surface and penetrating into the sediment. This would lead to more accurate time series

simulation. However, we demonstrated through comparing measured and simulated time series and good agreement with measured time series is demonstrated.

This angle dependent waveform distortion suggests that the different incident angles and their resultant phase shift each contain different information about a geoacoustic parameter. Hence, it could be considered that the ways to take advantage of these different phases in some kind of combination, such as Broadband Matched Filed Processing [11].

References

1. H. Medwin, C. S. Clay, "Fundamentals of acoustical oceanography," Academic press, Boston, 44-45, 1997.
2. I. Tolstoy, "Phase changes and pulse deformation in acoustics," *J. Acoust. Soc. Am.*, **44**, 675-683, 1968.
3. C. T. Tindle, "Ray calculations with beam displacement," *J. Acoust. Soc. Am.*, **73**, 1581-1586, 1983.
4. E. K. Westwood and P. J. Vidmar, "Eigenray finding and time series simulation in a layered-bottom ocean," *J. Acoust. Soc. Am.*, **81**, 912-924, 1987.
5. C. B. Officer, "Introduction to the theory of sound transmission," McGraw-Hill Book Co., Inc., New York, 108, 1958.
6. B. F. Cron, and A. H. Nuttall, "Phase distortion of a pulse caused by bottom reflection," *J. Acoust. Soc. Am*, **37**, 486-492, 1965.
7. L. B. Jackson, "Signals, systems, and transforms," Addison-Wesley Publishing Company, Reading, Massachusetts, 61-62, 1991.
8. J. B. Bowlin, "Ocean acoustical ray-tracing software ra y" Woods Hole Oceanographic Institution Technical Report No. 93-10 (WHOI-93-10), Woods Hole Oceanographic Institution, 1992.
9. Korea Institute of Geology, Mining & Materials "Submarine geological map of Korean continental shelf," Series VIII, 1993.
10. E. L. Hamilton, "Geoacoustic modeling of the seafloor," *J. Acoust. Soc. Am.*, **68**, 1313-1340, 1980.
11. A. Tolstoy, "Matched field processing for underwater acoustics," World Scientific, London, 181, 1993.

[Profile]

• Jooyoung Hahn

Jooyoung Hahn received the B.S and M.S degrees in Earth and Marine Sciences in 1997 and 1999, respectively, from Hanyang University, Korea. He is currently a Ph. D student in Earth and Marine Sciences in Hanyang University.

• Seongwook Lee

The Journal of the Acoustical Society of Korea, Vol. 21, No. 5.

• Jungyul Na

Jungyul Na received the B.S. degrees in astronomy and meteorology in 1968 from Seoul National University, Korea, and the M.S and Ph. D. degree in oceanography in 1973 and 1976, respectively, from Florida State University, Florida. He is currently a Professor in the Department of Earth and Marine Sciences and Director of Institute of Natural Science and Technology at Hanyang University, Ansan, Korea. His current research interests include boundary scattering and ocean acoustic Tomography. Dr. Na has also served as the president of the Acoustical Society of Korea from 1995 to 1998.